

PACS numbers: 68.55.J, 73.61.GA, 78.66.HF

**EFFECT OF ANNEALING ON STRUCTURAL, OPTICAL AND ELECTRICAL BEHAVIOURS OF WO<sub>3</sub> THIN FILMS PREPARED BY PHYSICAL VAPOUR DEPOSITION METHOD**

**Sunita Keshri<sup>1</sup>, Ashutosh Kumar<sup>1</sup>, Debdulal Kabiraj<sup>2</sup>**

<sup>1</sup> Department of Applied Physics, Birla Institute of Technology  
Mesra, Ranchi-835215, Jharkhand, India  
E-mails: [s\\_keshri@bitmesra.ac.in](mailto:s_keshri@bitmesra.ac.in), [sskeshri@rediffmail.com](mailto:sskeshri@rediffmail.com)

<sup>2</sup> Inter University Accelerator Centre,  
New Delhi, India

*The effect of annealing on structural, optical and electrical properties of tungsten oxide (WO<sub>3</sub>) thin films has been investigated. WO<sub>3</sub> films has been deposited on unheated corning glass and silicon substrates by physical vapour deposition, followed by annealing at temperatures 3000 °C and 5000 °C for 1 h in oxygen atmosphere. The as grown WO<sub>3</sub> film is amorphous whereas the annealed films show monoclinic crystalline behaviour. It has been observed that the films annealed at 3000 °C for 1 h had low surface roughness, good adhesion, high optical transmittance (upto 65 %) in the visible-infrared spectral range and good photoluminescence property in blue wavelength range. It is found from the transmittance spectra that the absorption edge is slightly shifted towards the longer wavelength region for the films annealed at higher temperatures. The present data could help to develop general strategies for the improvement of electrochromic and sensor devices based on WO<sub>3</sub> film.*

**Keywords:** THIN FILM, ABSORPTION COEFFICIENT, ELECTROCHROMIC BEHAVIOUR, PHOTOLUMINISCENCE, CONDUCTIVITY.

(Received 04 February 2011)

## 1. INTRODUCTION

Electrochromic devices are of interest for a wide range of applications and commercial activities are being started up. In particular, energy-efficient windows with variable solar and luminous transmittance are able to reduce the influx of solar energy into a building. This will lead to large reductions in the need for cooling and air conditioning in warm and temperate climates. In recent years, tungsten oxide films have been the focus of extensive scientific investigations due to their outstanding electrochromic properties [1]. Depending on the deposition conditions and techniques, films may present considerably different structural, optical and electrical behaviours. These films also have wide applications as gas sensors [2] and electro catalysis [3].

The purpose of this work is to deposit the material by physical vapour deposition technique and to optimize the formation of smooth nanocrystalline WO<sub>3</sub> films without delaminating from the substrate. The investigations so far carried out by us show that the films can be deposited with a good adhesion to both glass and silicon substrates. In this paper, we have systematically investigated the change of crystallinity, structural, optical and electrical properties of as-deposited WO<sub>3</sub> films and the films annealed at different temperature.

## 2. EXPERIMENTAL PROCEDURE

WO<sub>3</sub> films were deposited on the unheated corning glass and n-type Si (100) substrates by the e-beam evaporation of high-purity WO<sub>3</sub> powder (99.99 %) taken in water cooled copper crucible. The substrates were cleaned with trichloroethylene, isopropanol, acetone and deionized water before introducing it into the evaporator. The distance between the source to the substrates was ~ 20 cm and the base pressure in the evaporator was  $1 \times 10^{-8}$  Torr. Deposition rate was maintained as 1E/s with the help of a quartz crystal balance, and the thickness of all samples was set as 200 nm. These WO<sub>3</sub> films were annealed at 3000 °C and 5000 °C for 1 h in oxygen atmosphere with temperature ramp of 20 °C/min. The appearance of as-deposited film (a-WO<sub>3</sub>) was reddish, after annealing its colour changes to bluish.

Crystallographic structure of the specimen was examined at room temperature by a Philips diffractometer using CuK<sub>α</sub> radiation for the range  $200 \leq 2\theta \leq 800$  with step size of 0.02. The infrared (IR) transmission spectra were studied at room temperature by PerkinElmer Fourier transform infrared (FTIR) spectrometer (Spectrum 1000). Data was taken in attenuated total reflection mode. The surface morphology of the samples was obtained by JEOL scanning electron microscope (SEM); equipped with Oxford INCA energy dispersive X-ray (EDX) spectrometer. Photoluminescence (PL) spectrum was recorded with the help of HORIBA PL spectrometer, where a Xenon lamp was used as photon source. Electrical property of WO<sub>3</sub> film was measured by four-probe method with the help of Keithly 4200 source meter.

## 3. RESULTS AND DISCUSSION

### 3.1 Structural behavior

The SEM images of WO<sub>3</sub> films grown on Si substrate are shown in Fig. 1 a-c. The effect of temperature on the surface morphology of WO<sub>3</sub> films is remarkable. Prominent grains cannot be observed for a-WO<sub>3</sub> films even at very high magnifications. This observation is in agreement with the XRD results indicating the complete amorphous nature of the a-WO<sub>3</sub> films. The small dense particles, almost spherical in shape can be noticed in SEM image for WO<sub>3</sub> films annealed at 3000 °C and 5000 °C. The WO<sub>3</sub> films continue to show preferred growth along with an increase in average particle size with increasing temperature. However, grain distribution with proper adhesion is observed for the films annealed at 3000 °C.

In Fig. 2, IR spectra have been shown in the range 650-3500 cm<sup>-1</sup> for a-WO<sub>3</sub> and annealed films. The films show a broad peak in the range 1000-1800 cm<sup>-1</sup>. Peaks in the range 600-900 cm<sup>-1</sup> and 2250-2350 cm<sup>-1</sup> are also observed, almost in agreement with some previous results [4-5]. Peaks become more prominent as temperature increases.

Fig. 3 shows the X-ray diffractograms of WO<sub>3</sub> thin films on Si substrate. The XRD data shows that the structure of a-WO<sub>3</sub> film is amorphous. After annealing at 3000 °C and 5000 °C in oxygen atmosphere the crystallinity of film is improved [6]. After annealing the films show monoclinic phase described by space group P21/C (14) and lattice parameters are:  $a = 5.2610 \pm 0.0000$  Å,  $b = 5.1358 \pm 0.0189$  Å,  $c = 7.6500 \pm 0.0000$  Å and  $\beta = 92.051$ . The XRD pattern contains a peak corresponding to Si-substrate at  $2\theta \sim 67.79^\circ$ .

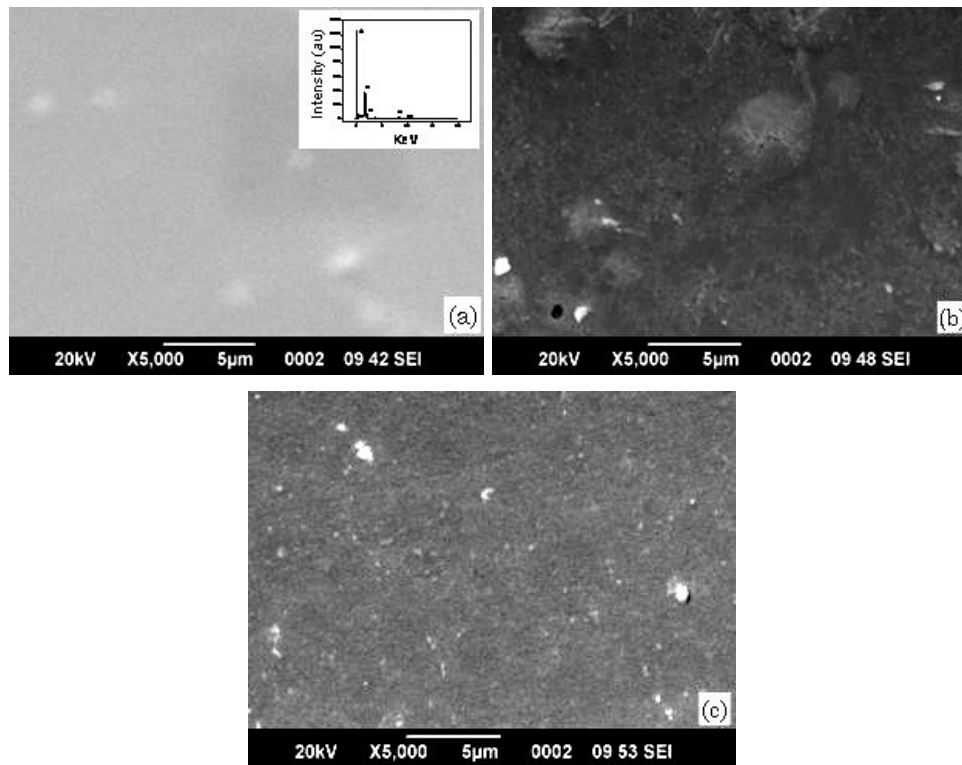


**Fig. 1** – SEM images of  $WO_3$  films: unannealed (a), annealed at 300 °C (b) and 500 °C (c). Inset of Fig. 1(a) shows EDX result of unannealed film

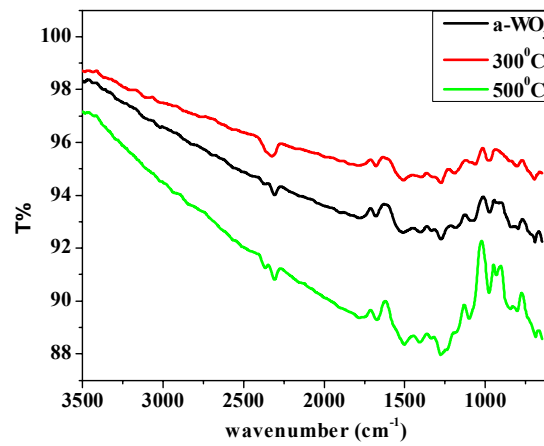


**Fig. 2** – FTIR results of  $a-WO_3$  and annealed films

The average crystalline size,  $D$  was determined by the Scherer method [7];

$$D = S\lambda/\beta\cos\theta, \quad (1)$$

where the Scherer constant,  $S = 0.9$ ,  $\lambda$  is the wavelength of the incident radiation,  $\beta$  is the full width half maximum intensity, and  $\theta$  is the Bragg angle corresponding to the peak being considered. The estimated average crystallite size is 40.32 and 47.60 nm for film annealed at 300 °C and 500 °C respectively. Hence in agreement with SEM results, these data also show that grain growth occurs with the increase of annealing temperature.

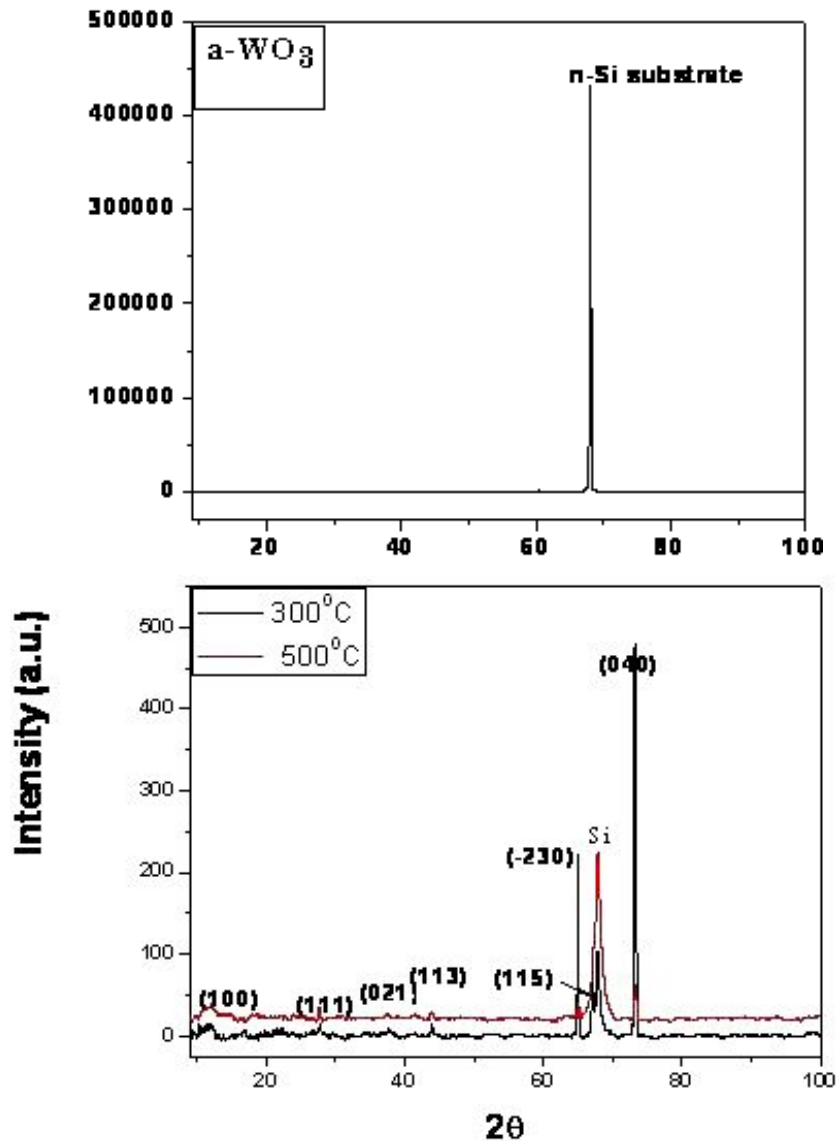


Fig. 3 – X-ray diffraction data for  $a\text{-WO}_3$  and annealed films

### 3.2 Optical behavior

Fig. 4 shows the optical transmission spectra of a-WO<sub>3</sub> and annealed films on glass substrate. The a-WO<sub>3</sub> film is transparent in the visible infrared spectral range with transmittance upto ~ 79 %; its transmittance decreases sharply at the wavelength ~ 370 nm due to the fundamental near absorption edge. The oscillations in the transmission spectra are caused by optical interference. Spectral transmittance of as deposited film to annealed film slightly decreases with increase in the annealing temperature. This may be because of the fact that although annealing causes improvement in crystallinity of the films, but it simultaneously increases the defect density. It is also observed that the absorption edge is slightly shifted towards the longer wavelength region for the films annealed at higher temperatures. The shift in absorption edge towards longer wavelength region has been assigned to the colouration effect of the films [8, 9] and is caused by a disappearance of short W=O bonds for the crystalline structures. [10]

This may be noted that WO<sub>3</sub> is an indirect semiconductor and the optical band gap of these films can be determined by considering the indirect transition between 2p electrons from the valence band of oxygen and the 5d conduction bands of tungsten using Tauc's relation [11] given as

$$(\alpha h\nu)^r = A(h\nu - E_g) \quad (2)$$

where  $A$  is a constant,  $h\nu$  is the incident photon energy,  $E_g$  is the optical energy band-gap, and  $\alpha$  is the absorption coefficient, which is obtained near the absorption edge from the transmittance,  $T$  using the equation

$$\alpha = \frac{1}{d} \ln\left(\frac{1}{T}\right) \quad (3)$$

where  $d$  is the thickness of the film. For indirect transitions the exponent takes the value  $r = 1/2$ . Thus the optical energy band-gap of WO<sub>3</sub> films deposited at different temperature was determined by plotting  $(\alpha h\nu)^{1/2}$  versus the incident photon energy ( $h\nu$ ), as shown in Fig. 5. The optical energy band-gap for as grown amorphous WO<sub>3</sub> film is found to be 3.41 eV, whereas the optical energy band gap for the crystalline films annealed at 300 °C and 500 °C has been calculated as 3.28 eV and 3.05 eV respectively. The results are in agreement with the previously reported data [12].

The PL spectra of the a-WO<sub>3</sub> and annealed films were measured using Xe lamp as the excitation source at room temperature; Fig. 6 shows the corresponding emission spectra. The emission peak of the as-deposited film consists of UV emissions and blue emissions. Emission at 467 nm appears for the Xe (source) lamp. It may be noted that the blue emission of this case can be attributed to the indirect band-band transition of WO<sub>3</sub> whereas the UV emission arise from the defect states of WO<sub>3</sub> [13-14]. After annealing at 300 °C, the blue emission becomes prominent which however not prominently observed for the film annealed at 500 °C. The results indicate that the film annealed at 300 °C show good PL spectra along with considerably good optical transmittance (~ 65 %) in the blue spectral range.

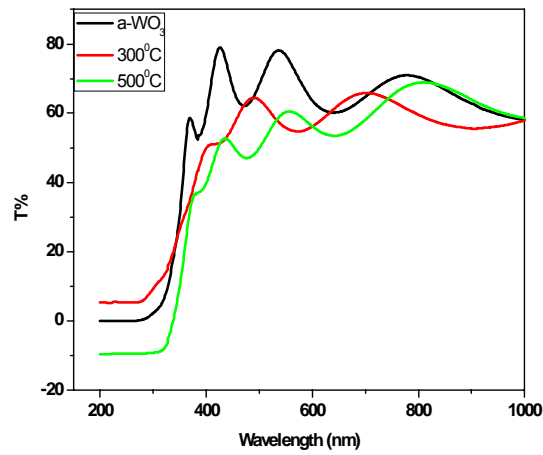


Fig. 4 – The spectral transmittance for  $a\text{-WO}_3$  and films annealed at 300 °C and 500 °C

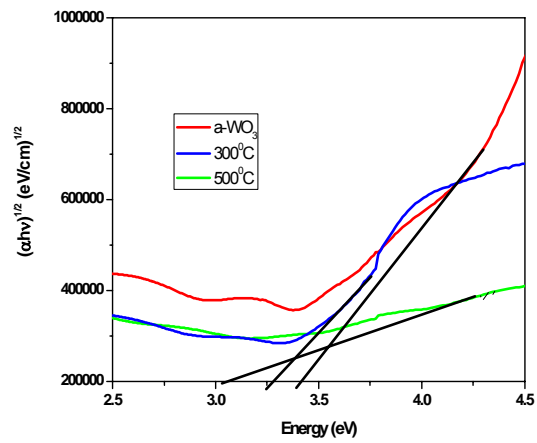


Fig. 5 – Plot of  $(\alpha h\nu)^{1/2}$  vs.  $(h\nu)$  for  $a\text{-WO}_3$  and films annealed at 300 °C and 500 °C

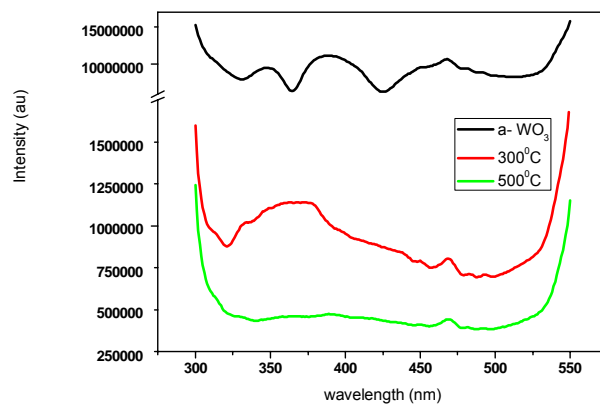


Fig. 6 – Photoluminescence spectra of  $a\text{-WO}_3$  and annealed films at 300 °C and 500 °C

### 3.3 Electrical Behaviour

The electrical conductivity,  $\sigma$ , as a function of temperature for unannealed and annealed  $\text{WO}_3$  films are shown in Fig. 7. It is observed that conductivity increases exponentially with increasing temperature, which could be attributed to the negative temperature coefficient of resistance and semiconducting nature of the  $\text{WO}_3$ . The figure shows that conductivity of the annealed films is larger. This is because with the increase in annealing temperature, grain size increases resulting in a decrease in grain boundaries and associated impedance to the flow of charge carriers [15]. Such a behavior is favourable for gas sensor applications of these films [16].

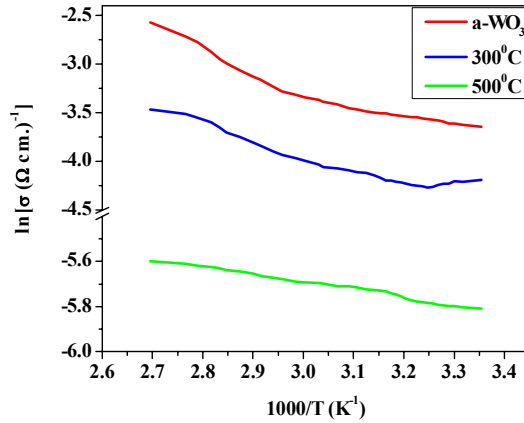


Fig. 7 – Temperature-dependent dc conductivity of  $\text{WO}_3$  thin films

## 4. CONCLUSION

The investigations so far carried out by us show that  $\text{WO}_3$  thin films prepared by physical vapor deposition method using e-beam present good adhesion to both glass and Si substrates. The transformation of amorphous to polycrystalline nature of the films was observed when we increase the annealing temperature. Post growth annealed samples have been characterized by XRD, FTIR, SEM, optical transmittance and PL spectroscopy. The nanocrystalline nature of  $\text{WO}_3$  films prepared at different annealing temperatures is evident from the XRD and SEM results reported here. Formation of smooth polycrystalline  $\text{WO}_3$  films without delamination from the substrates has been found by annealing at 300 °C. This film shows the best optical and electrical response due to improved crystallinity and enhanced light emission in the blue-wavelength region. We believe that these preliminary characteristic observations on the  $\text{WO}_3$  films will be helpful to explore the device performance of the films for electrochromic, gas sensors and smart window applications.

The authors would like to acknowledge UGC–DAE Consortium for Scientific Research, Kolkata Centre, India, for financial assistance. The authors are thankful to the members of Central Instrumentation Facility Lab, Birla Institute of Technology, Mesra for providing SEM and EDX facilities. For the work of XRD the members of Experimental Condensed Matter Physics Division of Saha Institute of Nuclear Physics are hereby acknowledged by the authors.

## REFERENCES

1. C.G. Granqvist, P.J. Gellings, H.J.M. Bouwmesster (Eds.), *The CRC Handbook of Solid State Electrochemistry* (Cleveland, Ohio, CRC Press, Inc.: 1997).
2. S.-H. Lee, H.M. Cheong, P. Liu, D. Smith, C.E. Tracy, A. Mascarenhas, J.R. Pitts, S.K. Deb, *J. Appl. Phys.* **88**, 3076 (2000).
3. J.F. Roland, F.C. Anson, *J. Electroanal. Chem.* **336**, 245 (1992).
4. N. Sharma, M. Deepa, P. Varshney, S.A. Agnihotry, *Thin Solid Films* **401**, 45 (2001).
5. M. Deepa, T.K. Saxena, D.P. Singh, K.N. Sood, S.A. Agnihotry, *Electrochim. Acta* **51**, 1974 (2006).
6. A.Z. Sadek, H. Zheng, M. Breedon, V. Bansal, S. K. Bhargava, K. Latham, J. Zhu, L. Yu, Z. Hu, P.G. Spizzirri, W. Wlodarski, K. Kalantarzadeh, *Langmuir* **25**, 9545 (2009).
7. A.A. Joraid, *Curr. Appl. Phys.* **9**, 73 (2009).
8. K.J. Patel, C.J. Panchal, V.A. Kheraj, M.S. Desai, *Mater. Chem. Phys.* **114**, 475 (2009).
9. G.R. Jafari, A.A. Saberi, R. Azimirad, A.Z. Moshfegh, S. Rouhani, *J. Stat. Mech.* **17**, P09017 (2006).
10. X. Sun, H. Cao, Z. Liu, J. Li, *Appl. Surf. Sci.* **255**, 8629 (2009).
11. M.G. Hutchins, O. Abu-Alkhair, M.M. El-Nahass, K. Abd El-Hady, *Mater. Chem. Phys.* **98**, 401 (2006).
12. C. Ng, C. Ye, Y.H. Ng, R. Amal, *Cryst. Growth Des.* **10**, 3794 (2010).
13. J. Diaz-Reyes, R.J. Delgado-Macuila, V. Dorantes-Garcia, A. Perez-Benitez, J.A. Balderas-Lopez, J.A. Ariza-Ortega, *Mater. Sci. Eng. B* **174**, 182 (2010).
14. J. Wang, P.S. Lee, J. Ma, *J. Cryst. Growth* **311**, 316 (2009).
15. R.S. Vemuri, K. Kamala Bharathi, S.K. Gullapalli, C.V. Ramana, *Appl. Mater. Interfaces* **9**, 2623 (2010).
16. M.G. Hutchins, O. Abu-Alkhair, M.M. El-Nahass, K. Abdel-Hady, *J. Phys.: Condens. Matter* **18**, 9987 (2006).